

# Monte Carlo calculation for systems consisting of several coordinate patches

Claus Vohwinkel

*Supercomputer Computations Research Institute, The Florida State University,  
Tallahassee, FL 32306, USA*

October 17, 1994

## Abstract

I investigate the time step dependence of Monte Carlo simulations for coordinate-spaces consisting of several patches. It is shown that a naive kinetic term does not necessarily converge to the same spectrum as a Hamiltonian calculation. Then an improved kinetic term is presented which allows one to connect the Monte Carlo and Rayleigh-Ritz results of intermediate volume SU(2) gauge theory.

## 1 Introduction

There have been two approaches in the intermediate volume calculation of SU(2) gauge theory: The Hamiltonian approach [1], which is a Rayleigh-Ritz analysis of an effective Hamiltonian. and the Lagrangian approach [2][3] which is a Monte Carlo simulation of an effective Lagrangian. For a review of most of the work done in this area see [4]. Although both approaches are formally equivalent [5], the numerical data obtained does not agree. A study of the Lagrangian approach using smaller time steps did not improve the results [6].

In both approaches the coordinate space consists of 8 compact patches, which correspond to equivalent vacua. Basically these patches are spheres and tunneling from one sphere into another one can take place via any point

of the boundary of the sphere. This means, that in flat space, we cannot form a single large patch by joining all the patches together. The idea, that this kind of geometry is responsible for the difference of the Lagrangian and Hamiltonian results, is very tempting. Indeed, the disagreement in the energy spectrum is still present, when one switches off the potential energy. One can therefore study the simpler case of a free particle moving in the same geometry, which allows one to use analytical methods. This is carried out in section 2. After having understood the reason for the disagreement, one can change the kinetic term in the Lagrangian approach to match the Hamiltonian approach. A procedure to do so and some Monte Carlo results are given in section 3. Finally section 4 contains some conclusions.

## 2 A toy model

The model without the potential energy factorizes into 3 wave functions. For the analysis attempted here, it is sufficient to describe one of these wave functions: Our toy model consists of a free particle moving in two spheres, each of radius  $\pi$ . The obvious choice of coordinates are spherical coordinates and an integer  $k = 0, 1$ , giving the sphere in which the particle is:

$$\tilde{\psi} = \tilde{\psi}(r, \theta, \varphi, k). \quad (1)$$

The spheres touch each other at their boundary. (One can picture this a two spheres occupying the same space.) For the particle to move from the interior of one sphere to the other one, it has to move to any point on the boundary  $r = \pi$  where it changes to the other sphere and then moves on inward.

Due to the symmetry of the problem the eigenfunctions will be either symmetric or anti-symmetric under interchange of the spheres. One can therefore describe the wave function by its wave function  $\psi$  in one sphere and its symmetry type.

For the anti-symmetric wave functions the boundary condition at  $r = \pi$  is unambiguous:

$$\psi(r, \theta, \varphi) = 0. \quad (2)$$

For the symmetric wave function the choice is not as clear cut. Due to the measure one should however look at  $r\psi(r, \theta, \varphi)$  instead of  $\psi(r, \theta, \varphi)$ . One can

select a basis  $B(b)$  by requiring

$$\left. \frac{\partial}{\partial r} \log(r\psi(r, \theta, \varphi)) \right|_{r=\pi} = b, \quad (3)$$

for a given  $b$ . In the original problem the angular variables could not be observed, and the obvious choice was  $b = 0$ . Here, however, one is free to choose any  $b$ . The eigenfunctions are given by

$$\psi_{ilm}(r, \theta, \varphi) = j_l(\alpha_i r) Y_{lm}(\theta, \varphi) \quad (4)$$

where  $\alpha_{i-1}$  is the  $i$ 'th zero (2) or (3). That these functions form a basis for any  $b$ , follows from the orthogonality properties of the Bessel functions.

In the Lagrangian approach, or to be more precise the Monte Carlo calculation with finite time step  $\epsilon$  [3], the configurations are described by a spatial coordinates  $\vec{r}(t)$  and a coordinate  $k(t) \in \{0, 1\}$  which describes in which sphere the particle is. The measure is flat in  $\vec{r}$  and one possible kinetic term is given by [5]:

$$T_{kin}(\vec{r}(t), \vec{r}(t+\epsilon), \Delta k) = \frac{1}{2\epsilon^2} (\vec{r}(t) - \vec{r}(t+\epsilon))^2 + \Delta k \frac{(\pi^2 - r^2(t))(\pi^2 - r^2(t+\epsilon))}{2\pi^2\epsilon^2}, \quad (5)$$

where  $\Delta k = |k(t) - k(t+\epsilon)|$ . In [3] it was proposed that, for  $\Delta k = 1$  one should calculate the geodesic distance  $d_g$  between  $c(t)$  and  $c(t+\epsilon)$  and use

$$T_{gd} = \frac{1}{2\epsilon^2} d_g^2. \quad (6)$$

It was argued that both kinetic terms should give the same continuum limit, but (6) should have smaller finite  $\epsilon$  effects. Unfortunately the geodesic distance is the root of a quartic equation which makes analytic calculations hard. I shall therefore restrict a transfer matrix analysis to the Lagrangian (5). Later on I shall do a numerical comparison with (6).

## 2.1 Transfer matrix calculations

One can calculate the energy spectrum for finite time step  $\epsilon$  by means of the transfer matrix approach. To this end let me calculate the transfer matrix between two wave functions  $\psi$  and  $\phi$

$$T_{\tilde{\psi}, \tilde{\phi}} = \sum_{k_1, k_2=0}^1 \int d\vec{r}_1 d\vec{r}_2 \tilde{\psi}(\vec{r}_1, k_1) \tilde{\phi}^*(\vec{r}_2, k_2) K(\vec{r}_1, \vec{r}_2, |k_1 - k_2|), \quad (7)$$

where

$$K(\vec{r}_1, \vec{r}_2, \Delta k) = \frac{1}{\sqrt{2\pi\epsilon}} \exp[-\epsilon T_{kin}(\vec{r}_1, \vec{r}_2, \Delta k)]. \quad (8)$$

Due to the symmetry we can split up the transfer matrix into an interior ( $T_0$ ) and exterior ( $T_1$ ) part:

$$T(\tilde{\psi}, \tilde{\phi}) = \begin{cases} T^0(\psi, \phi) + T^1(\psi, \phi) & , \psi \text{ and } \phi \text{ symmetric} \\ T^0(\psi, \phi) - T^1(\psi, \phi) & , \psi \text{ and } \phi \text{ antisymmetric} \\ 0 & , \text{ otherwise} \end{cases} \quad (9)$$

with

$$T^k(\psi, \phi) = \int d\vec{r}_1 d\vec{r}_2 \psi(\vec{r}_1) \phi^*(\vec{r}_2) K(\vec{r}_1, \vec{r}_2, k), \quad (10)$$

where  $\psi$  and  $\phi$  are wave functions of the form (4). Due to the spherical symmetry of the problem, wave functions with different angular momentum do not mix and one has

$$T^k(\psi_{ilm}, \phi_{jpq}) = T_{ij,l}^k \delta_{lp} \delta_{mq}. \quad (11)$$

## 2.2 Expansion for small time steps

The matrix elements can be calculated as a series in  $\epsilon^{1/2}$ . I shall restrict myself here to the more interesting case of the symmetric sector. Also I shall give results for  $l = 0$  only and drop the  $l$  and  $m$  references and angular variables from the notation. One obtains for the diagonal elements:

$$T_{ii} = e^{-\frac{1}{2}a_i^2\epsilon} \left[ 1 + \frac{a_i^2\epsilon}{12\pi(\pi b^2 - b + \pi a_i^2)} (a_i^4\epsilon - 6a_i^2\epsilon - 12\pi b + 6) \right] + O(\epsilon^{3/2}). \quad (12)$$

(Note that  $a_i$  can be arbitrary large, that is  $a_i^2\epsilon$  is not necessarily small.) For the off-diagonal elements,  $a_i$  of order 1 and  $a_j$  arbitrary, one has

$$T_{ij} = -N_i N_j (-1)^{i-j} \left( \frac{2\pi b + 1}{\pi^2 a_j^2} + \frac{a_j^2\epsilon + 2\pi b + 1}{\pi^2 a_j^2} e^{-\frac{1}{2}a_j^2\epsilon} \right) + O(\epsilon^{3/2}), \quad (13)$$

with

$$N_i = \sqrt{\frac{\pi a_i}{\pi b^2 - b + \pi a_i^2}}. \quad (14)$$

For  $a_j$  of order 1 one will need the next order in  $\epsilon^{1/2}$  as well, and the matrix element for both,  $a_i$  and  $a_j$  of order 1 is given by:

$$T_{ij} = -(-1)^{i-j} N_i N_j \left( \frac{(2\pi b - 1)\epsilon}{2\pi^2} + \frac{\sqrt{8}(\pi b - 1)^2 \epsilon^{3/2}}{3\pi^{7/2}} \right) + O(\epsilon^2). \quad (15)$$

Let us assume we can do perturbation theory around  $\Psi = \psi_i(r)$ . The first order corrections to the groundstate wave function are

$$\langle \psi_j \Psi \rangle = \frac{T_{ji}}{E_i - E_j}. \quad (16)$$

For small  $a_j$  one has

$$\langle \psi_j \Psi \rangle = (2\pi - b)O(1) + O(\epsilon^{1/2}). \quad (17)$$

and for  $a_j \geq O(1/\sqrt{\epsilon})$  one has

$$\langle \psi_j \Psi \rangle_l = -\frac{(-1)^{i-j} a_0}{\pi^{3/2} \sqrt{\pi b^2 - b + \pi a_0^2}} \frac{(2\pi b + 1)e^{\frac{1}{2}a_j^2 \epsilon} - a_j^2 \epsilon - 2\pi b - 1}{a_j^2 (e^{\frac{1}{2}a_j^2 \epsilon} - 1)} \quad (18)$$

Note that for  $b = -\frac{1}{2\pi}$  the corrections (18) to the wave function vanish exponentially, once  $a_j^2 > \epsilon$ , whereas for all other choices for  $b$  they only vanish as  $a_j^{-2}$ . Thus, for any finite  $\epsilon$  we expect the correct wave function to obey boundary conditions (3) with  $b = -\frac{1}{2\pi}$ , but the region where the slope of the wave function becomes compatible with this b.c. becomes more narrow as  $\epsilon$  decreases. In this simple argument I ignored the fact that in the basis  $b = -\frac{1}{2\pi}$  the first  $O(1/\sqrt{\epsilon})$  trial functions contribute substantially to the true groundstate wave function. Later on I shall give a more rigorous derivation of the boundary condition.

From eq. (17) one sees, that the only basis were one is allowed to do perturbation theory (in  $\epsilon^{1/2}$ ) is  $b = \frac{1}{2\pi}$ .

For this choice of  $b$  the matrix element (18) reads:

$$\langle \psi_j \Psi \rangle_l = -\frac{2a_i(-1)^{i-j}}{\pi \sqrt{4\pi a_i^2 - 1}} \frac{2e^{\frac{1}{2}a_j^2 \epsilon} - a_j^2 \epsilon - 2}{a_j^2 (e^{\frac{1}{2}a_j^2 \epsilon} - 1)} \quad (19)$$

For  $a_j < O(\epsilon^{-1/4})$  the dominant contribution comes from the  $O(\epsilon^{1/2})$  term in (17):

$$\langle \psi_j \Psi \rangle_s = \frac{4\sqrt{2}(-1)^{i-j} a_i a_j \epsilon^{1/2}}{3\pi^{3/2}(a_j^2 - a_i^2) \sqrt{(4\pi^2 a_i^2 - 1)(4\pi^2 a_j^2 - 1)}}. \quad (20)$$

Let me calculate the sum over all matrix element squared to see whether perturbation theory can be applied to this basis. From eq. (3) one has  $a_j - a_{j-1} \approx 1$ , and because we are only interested in the order of the correction, we can replace the sum by an integral. Eq. (19) gives a contribution

$$\sum_{j \neq i} \langle \psi_j \Psi \rangle_s^2 \approx \epsilon^{3/2} \int_0^\infty da \frac{2e^{\frac{1}{2}a^2} - a^2 - 2}{a^2(e^{\frac{1}{2}a^2} - 1)} = O(\epsilon^{3/2}), \quad (21)$$

whereas eq. (20) contributes

$$\sum_{j \neq i} \langle \psi_j \Psi \rangle_s \approx \int_1^\infty da \frac{\epsilon}{a^2} = O(\epsilon). \quad (22)$$

Thus, corrections to the groundstate wave function vanish as  $\epsilon \rightarrow 0$ , and one can indeed do perturbation theory about  $\epsilon = 0$ .

One is now in a position to determine the energy spectrum  $E_i = -\log(T_{ii})/\epsilon$  of the Lagrangian. I am using the basis  $b = \frac{1}{2\pi}$  and restrict myself to the low-lying states  $a_i = O(1)$ .

In addition to the diagonal element  $T_{ii}$  one needs the second order correction

$$\Delta V_i = \sum_{j \neq i} \Delta V_{ij} = \sum_{j \neq i} \frac{T_{ij} T_{ji}}{T_{ii} - T_{jj}}. \quad (23)$$

The only term contributing to  $O(\epsilon^{3/2})$  is

$$\Delta V_{ij} = \frac{4a_i^2 \epsilon^2}{\pi^2(4\pi^2 a_i^2 - 1)} \frac{\left( (2 + a_j^2 \epsilon) e^{-\frac{1}{2} a_j^2 \epsilon} - 2 \right)^2}{a_j^4 \epsilon^2 (1 - e^{-\frac{1}{2} a_j^2 \epsilon})} \quad (24)$$

For small  $j$  the contribution  $\Delta V_{ij}$  from (24) vanish as  $\epsilon^3$  and can be neglected. Therefore one can replace the sum over  $j$  by and integral over  $a$  to obtain

$$\Delta V_i = \frac{4a_i^2 \epsilon^{3/2}}{\pi^2(4\pi^2 a_i^2 - 1)} \int_0^\infty da \frac{\left( (2 + a^2) e^{-\frac{1}{2} a^2} - 2 \right)^2}{a^4 (1 - e^{-\frac{1}{2} a^2})}. \quad (25)$$

Together with the diagonal element  $T_{ii}$  up to  $O(\epsilon^{3/2})$

$$T_{ii} = e^{-\frac{1}{2}a_i^2\epsilon} + \frac{4a_i^2\epsilon^{3/2}}{3\sqrt{2}\pi^{3/2}(4\pi^2a_i^2 - 1)} + O(\epsilon^2), \quad (26)$$

one obtains for the energy

$$E_i = \frac{1}{2}a_i^2 - 0.274112\frac{a_i^2\sqrt{\epsilon}}{4\pi^2a_i^2 - 1}. \quad (27)$$

Eq. (3) gives  $a_0 = 0.3710096482\dots$ , and one gets for the groundstate energy:

$$E_0 = 0.06882408 - 0.0085092\sqrt{\epsilon}. \quad (28)$$

Using the same approach in the anti-symmetric sector one obtains for the energy of the lowest state

$$E_a = \frac{1}{2} + \frac{1}{2\pi^2}\epsilon. \quad (29)$$

Let me come back to the boundary conditions in the symmetric sector. We can confirm our previous analysis about the derivative at the boundary by calculating it in the basis  $b = \frac{1}{2\pi}$ . To this end let me write

$$\frac{\partial}{\partial r} \log(r\psi(r, \theta, \phi)) = \lim_{u \rightarrow 0} \frac{\Phi(\pi) - \Phi(\pi - u\sqrt{\epsilon})}{u\sqrt{\epsilon}\Phi(\pi)}, \quad (30)$$

where  $\Phi(r) = r\Psi_i(r, \theta, \phi)$ . Let me restrict myself to the case  $l = 0$ . Except for  $\psi_0$  the only relevant contribution come from large  $j$ , and one has:

$$\Phi(\pi) - \Phi(\pi - u\sqrt{\epsilon}) = \frac{\sqrt{8}a_i\sqrt{\epsilon}}{\pi^{3/2}\sqrt{4\pi^2a_i^2 - 1}} \left[ -\frac{u\pi}{2} - \int_0^\infty da \frac{\cos(au) - 1}{e^{\frac{1}{2}a^2} - 1} \right] \quad (31)$$

The integral in eq. (31) is of order  $u^2$  and its value can be ignored. One obtains for derivative

$$\frac{\Phi(\pi) - \Phi(\pi - u\sqrt{\epsilon})}{u\sqrt{\epsilon}\Phi(\pi)} = -\frac{1}{2\pi} + O(u). \quad (32)$$

Thus we arrive the previous result. Because the first correction in  $u$  is  $O(u)$  (as opposed to  $O(u\epsilon^{1/2})$ ), one has  $\Phi'(r)/\Phi(r) \approx -\frac{1}{2\pi}$  for  $|r - \pi| < \sqrt{\epsilon}$ . But further away from the boundary and small enough  $\epsilon$  the wave function becomes compatible with the lowest function of the  $b = \frac{1}{2\pi}$  basis.

Table 1: Rayleigh-Ritz results. Shown are the number of basis states  $n_b$  used in the Rayleigh-Ritz calculation, the groundstate energy  $E_0$ , the lowest state in the anti-symmetric sector  $E_a$  and the lowest  $l = 1$  state  $E_1$ . All  $E_1$  estimates were computed with 50 basis states.

$\epsilon$	$n_b$	$E_0(\epsilon)$	$E_a(\epsilon) - \frac{1}{2}$	$E_1(\epsilon)$
$2.0 \cdot 10^{-1}$	50	0.066552	$1.27270 \cdot 10^{-2}$	0.308909
$1.0 \cdot 10^{-1}$	50	0.066858	$5.92709 \cdot 10^{-3}$	0.306617
$5.0 \cdot 10^{-2}$	200	0.067272	$2.82432 \cdot 10^{-3}$	0.305885
$2.0 \cdot 10^{-2}$	300	0.067757	$1.08418 \cdot 10^{-3}$	
$5.0 \cdot 10^{-3}$	300	0.068256	$2.61903 \cdot 10^{-4}$	
$2.0 \cdot 10^{-3}$	400	0.068457	$1.03473 \cdot 10^{-4}$	
$2.0 \cdot 10^{-4}$	600	0.068706	$1.01993 \cdot 10^{-5}$	
$2.0 \cdot 10^{-5}$	800	0.068786	$1.01536 \cdot 10^{-5}$	

### 2.3 Rayleigh-Ritz and Monte Carlo results

Instead of expanding the matrix elements  $T_{ij}$  in a series in  $\epsilon^{1/2}$ , they can be calculated numerically (ignoring terms of order  $\exp[-2\pi^2/\epsilon]$ ) and used for a Rayleigh-Ritz analysis. The internal elements  $T_{ij}^0$  can be integrated analytically, while the external elements  $T_{ij}^1$  can be reduced to a one dimensional integral which has to be performed numerically. Due to the exponential fall-off of the matrix elements  $T_{ij}$  for large  $j$ , the basis  $b = -\frac{1}{2\pi}$  is best suited for this calculation. Depending on  $\epsilon$ , between 50 and 800 basis states were used. For the three largest  $\epsilon$ , the transfer matrix in the  $l = 1$  sector was calculated by means of a two dimensional numerical integral. The results for the vacuum  $E_0$ , the lowest anti-symmetric state  $E_a$ , and the lowest  $l = 1$  state  $E_1$  are given in table 1. From the results one can estimate the next term in the expansion of  $E_0(\epsilon)$  in term of  $\epsilon$ :

$$E_0(\epsilon) \approx 0.06882408 - 0.0085092\sqrt{\epsilon} + 0.007\epsilon \quad (33)$$

In figure 1 the Rayleigh-Ritz results as well as the two series are shown.

Using the data from table 1 one can calculate the mass gaps for the first antisymmetric state  $m_a$  and the first  $l = 1$  state  $m_1$ . I have also calculated



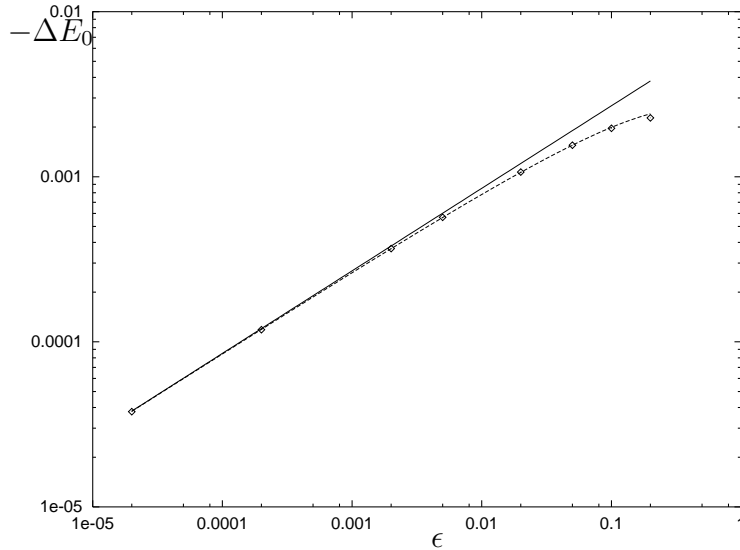


Figure 1: Comparison of the Rayleigh-Ritz calculation (diamonds), expansion up to  $\epsilon^{1/2}$  (solid line) and estimated expansion up to  $O(\epsilon)$  (dashed line) for the groundstate energy  $\Delta E_0 = E_0(\epsilon) - E_0(0)$ .

the mass gaps for these sectors by means of Monte Carlo simulation, using both kinetic terms, (5) and (6). Table 2 shows the results.

The data for the asymmetric state is also plotted in figure 2. One can see good agreement between the Rayleigh-Ritz calculation and the Monte Carlo simulation with kinetic term (5). From the data it seems however very unlikely that the results for the different kinetic terms converge at  $\epsilon = 0$ . In addition, a look at the groundstate wave function (which can be obtained from histograms in the MC calculation) shows a different behaviour for the two kinetic terms as well. This results comes as no surprise if one looks at a very simple case: In [3] it was shown that for  $\vec{r}(t)$  and  $\vec{r}(t + \epsilon)$  equal but in different patches, the kinetic term (5) becomes  $T_{kin} = (2\delta)^2(1 - \delta/(2\pi))^2$ , where  $\delta = \pi - r(t)$ . The geodesic distance for this configuration is exactly  $(2\delta)^2$ . If one follows terms of the form  $\delta^3$  through the small- $\epsilon$  expansion, one finds they contribute  $O(\epsilon)$  to the external matrix element. But this exactly the order which gives the zeroth order energy.

As mentioned earlier the geodesic distance is the solution of a quartic equation. Even for small  $\epsilon$ , configurations which have multiple zeroes of the

Table 2: Monte Carlo results for the toy model. The table shows Rayleigh-Ritz and Monte Carlo results for  $m_a$  and  $m_1$ .  $RR$  denotes the Rayleigh-Ritz calculation,  $MC$  the Monte carlo results obtained by using the kinetic term (5) and  $gd$  are the masses for the simulation with kinetic term (6).

$\epsilon$	$m_a$			$m_1$		
	$RR$	$MC$	$gd$	$RR$	$MC$	$gd$
0.05	0.435553	0.436(5)	0.336(4)	0.23862	0.2378(15)	0.2672(10)
0.10	0.439069	0.440(4)	0.338(2)	0.23976	0.2394(10)	0.2696(10)
0.20	0.446175	0.446(2)	0.341(2)	0.24236	0.2420(4)	0.2668(6)

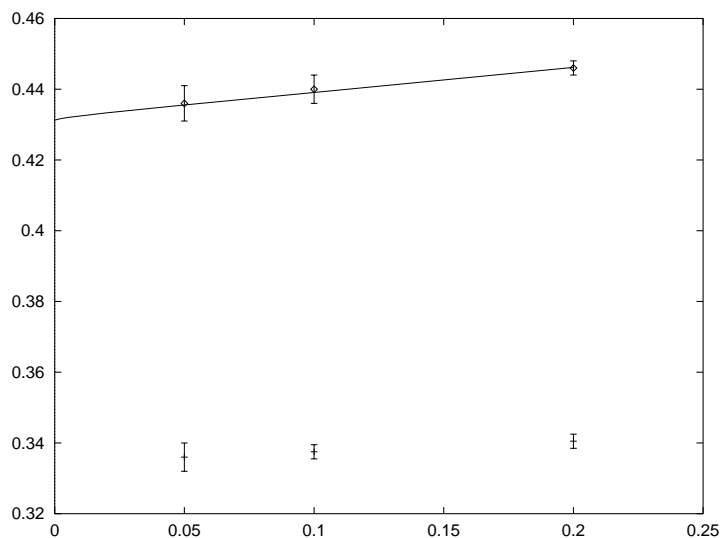


Figure 2: Results for  $m_a$ . The solid line is the Rayleigh-Ritz calculation, the diamonds are the Monte Carlo simulation using the kinetic term (5) and the crosses are the results for the kinetic term (6).

equation are not suppressed. The influence of these configurations is beyond the scope of this article, but I would suspect that they also contribute to the observed energy difference.

### 3 An improved kinetic term

Instead of using a kinetic term like (5), it is possible to use a kinetic term which will exactly reproduce the Hamiltonian result for the toy model. Again one would be free to tailor the kinetic term to any boundary condition (3). In order to make connection to the Rayleigh-Ritz results of [1], I choose  $b = 0$ . I make the Ansatz:

$$e^{-\epsilon L_{kin}(\vec{r}_1, \vec{r}_2, \Delta k)} = \sqrt{2\pi\epsilon}^3 \sum_{s=0}^1 \sum_{j,l=0}^{\infty} (-1)^{s\Delta k} j_l(\alpha_{slj}r_1) j_l(\alpha_{slj}r_2) P_l(c) e^{-\frac{1}{2}\alpha_{s,j}^2\epsilon}, \quad (34)$$

where  $c$  is the angle between  $\vec{r}_1$  and  $\vec{r}_2$  and  $\alpha_{0lj}$  and  $\alpha_{1lj}$  are chosen according to (3) and (2) respectively. For large enough  $\epsilon$  one can stop the sum at some values  $l_{max}$  and  $j_{max}$  without introducing a large error (compared to the statistical error of the MC-calculation). For  $\epsilon$  down to 0.15, I found  $l_{max} = 100$  and  $j_{max} = 40$  to be sufficient. Of course it is impracticable to calculate the sum at every update step of the Monte Carlo procedure. But one can tabulate the values and look them up during the actual calculation. To this end we notice that (34) depends on three continuous coordinates  $r_1, r_2$  and  $c$ . The influence from the boundary will be large only for  $\vec{r}_1$  and  $\vec{r}_2$  close the boundary. Otherwise

$$-\epsilon L_{kin}(\vec{r}_1, \vec{r}_2, 0) \approx -\frac{1}{2\epsilon}(r_1^2 + r_2^2 - 2r_1r_2c), \quad (35)$$

and configurations with  $\Delta k = 1$  and  $\vec{r}_1$  or  $\vec{r}_2$  away from the boundary are strongly suppressed. Therefore I chose to tabulate  $L_{kin}$  as a cubic spline interpolation  $S(r_1, r_2, c)$  in 3 dimensions, which is capable of describing (35) exactly. For spline interpolation the gridpoints do not have to be equally spaced (for a discussion of spline interpolation see for example [7]). A rough estimate suggest that the influence of the boundary, i.e. the deviation from the quadratic form (35) is of the order of  $\exp[-(\pi - r)^2/(2\epsilon)]$ . Therefore the gridpoints (in both r directions) are chosen according to the distribution

Table 3: Monte Carlo results using the improved kinetic term.

state	exact	MC
$A_1$	1.0	0.9985(15)
$A_2$	3.0	2.998(4)
$\epsilon$	0.375	0.373(2)
$p$	0.25637..	0.2563(6)

function

$$F(r) = \beta r + \operatorname{erf}(\pi/\sqrt{2\epsilon}) - \operatorname{erf}((\pi - r)/\sqrt{2\epsilon}), \quad (36)$$

where  $\beta$  is chosen to minimize the maximum error<sup>1</sup>. For the spline interpolation one needs to store for each gridpoint eight values:

$$S, \frac{\partial^2 S}{\partial r_1^2}, \frac{\partial^2 S}{\partial r_2^2}, \frac{\partial^2 S}{\partial c^2}, \frac{\partial^4 S}{\partial r_1^2 \partial r_2^2}, \frac{\partial^4 S}{\partial r_1^2 \partial c^2}, \frac{\partial^4 S}{\partial r_2^2 \partial c^2}, \frac{\partial^6 S}{\partial r_1^2 \partial r_2^2 \partial c^2}. \quad (37)$$

The eight quantities (37) can be calculated from (34). (The derivatives at the boundary which are needed to calculate (37) can also be obtained from eq. (34)). Once the spline table is set up the calculation of the kinetic energy takes about 200 floating point operations.

For the simulations I used a  $50^3$  grid. Due to the symmetry under  $r_1 \leftrightarrow r_2$  the size of the table is  $8 \times 2 \times 50^3/2$  numbers, which translates to 8 Mbytes when using IEEE double precision. The placement of the r-gridpoints are shown in figure 3. In figures 4 and 5 an estimate of the error  $|\exp[-\epsilon S] - \exp[-\epsilon L]|$  of the spline approximation to the Boltzmann weight is shown.

For all  $\epsilon$  used in the simulation the maximum absolute error was about  $10^{-8}$  and can be neglected against the statistical error of the simulation. Due to the Ansatz (34) the Monte Carlo calculation of the free particle should reproduce the Hamiltonian results for any value of  $\epsilon$ . In table (3) data for  $\epsilon = 0.6$  is given. Smaller  $\epsilon$  give the same results within errors, but need more CPU-time to obtain the same accuracy.

However, when one returns to the original problem there will be  $O(\epsilon^2)$  corrections, due to the potential energy term, and one has to estimate the

---

<sup>1</sup>if  $\beta$  is too small the interpolation starts to oscillate away from the boundary

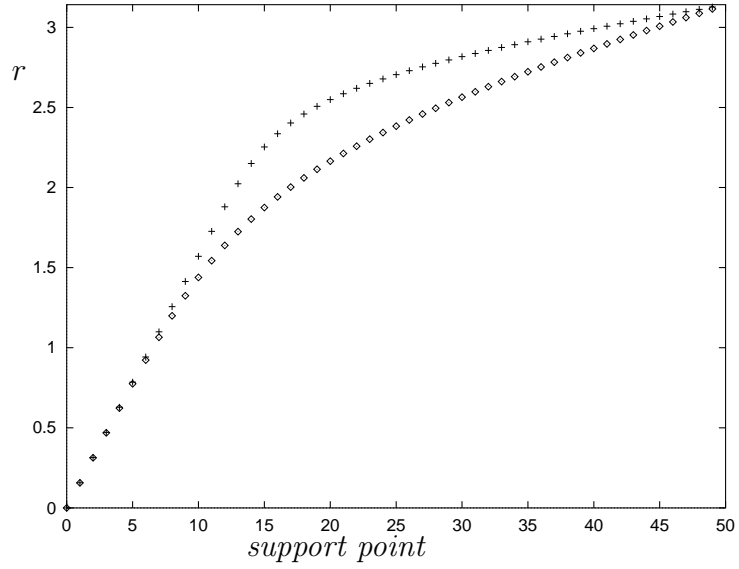


Figure 3: Location of support points for spline interpolation. Shown are the locations for  $\epsilon = 0.6$  (diamonds) and  $\epsilon = 0.15$  (crosses).

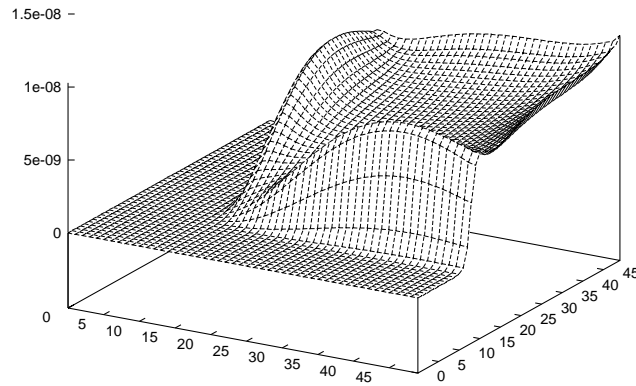


Figure 4: Absolute error of spline interpolation to the Boltzmann weight for both coordinates in the same sphere

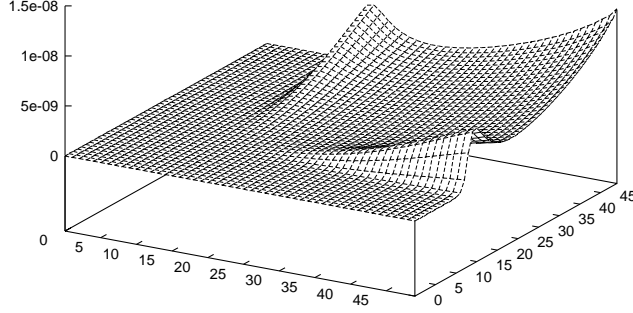


Figure 5: Absolute error of spline interpolation to the Boltzmann weight for the coordinates in different spheres

finite time step errors. It is therefore necessary to simulate the Lagrangian at different time steps  $\epsilon$ . To clarify the notation used for the results let me write the Lagrangian in its original form:

$$\tilde{\epsilon}L = \frac{1}{2}(g^{-2} + \alpha_1)\frac{(\Delta\vec{r})^2}{\tilde{\epsilon}} + \tilde{\epsilon}V(\vec{r}). \quad (38)$$

One can connect this form to a free particle and eq. (34) by writing the kinetic term as

$$\tilde{\epsilon}T_{kin} = \frac{1}{2}\frac{(\Delta\vec{r})^2}{a}. \quad (39)$$

This gives for the effective time step

$$\tilde{\epsilon} = a\left(\frac{1}{g^2} + \alpha_1\right), \quad (40)$$

which has to be used to calculate the mass gap from the correlation function. The kinetic energy term, however, has to be computed by using  $a$  for the time step in eq. (34). Monte Carlo simulations were performed for  $a = 0.15, 0.3, 0.6$  and  $g = 1.4, 1.8, 2.0$ . The results for various states are given in table (4),

which also contains an extrapolation down to  $a = 0$ . One finds excellent agreement for most states, indicating that the discrepancy of the previously published results is entirely due to the kinetic term.

## 4 Conclusions

The treatment of non-trivially connected coordinate spaces using Monte Carlo methods needs some care. There are basically two effects which hinder the MC approach with a naive kinetic term. Firstly one encounters corrections of the order of the square root of the time step, which require very small time steps and therefore large amounts of CPU time. Secondly, and more severe the conditions at the coordinate patch connection are not under control. Usually one would argue that the Monte Carlo approach will choose the correct boundary conditions. But if the connection of the patches is not simple, this argument is on very weak footing, and the boundary condition (and spectrum) preferred by the simulation depends on details of the kinetic term. The problem can be overcome by constructing a kinetic term which will match predetermined conditions at the boundary. In the case studied here, the term could be tabulated and used efficiently in a MC calculation. The improved kinetic term has no finite time step correction, and one is left with  $O(\epsilon^2)$  correction from the potential energy.

Using the improved kinetic term, I was able to reproduce the Rayleigh-Ritz results of [1] with the Lagrangian approach. Note that both approaches have the same degree of freedom in choosing the boundary conditions. In the original Lagrangian approach [3] the freedom of choice is not as obvious, because it is hidden non-trivially in the choice of sub-leading orders of the kinetic term.

Let me remark at this point that the transfer matrix approach of [8] is unrelated to the approach presented here, that is van Baal's result of small finite time step corrections does not contradict my findings.

## Acknowledgements

This research project was partially funded by the Department of Energy under contracts DE-FG05-87ER40319 and DE-FC05-85ER2500. Finally, I

Table 4: Masses for SU(2) small volume calculation. The values for  $a = 0.15, 0.3, 0.6$  are measurements. The  $a = 0$  column is the extrapolation to  $a = 0$  assuming an  $a^2$  dependence of the mass. Cont. is the result from the Hamiltonian approach [1]. For some states I was unable to extract the mass for  $a = 0.15$ , the corresponding entries are left blank.  $\epsilon, \epsilon_2$  and  $\epsilon_3$  are states with 1, 2 and 3 units of electric flux.  $A_1^+, E^+, T_2^+, A_1^-$  are IR of the cubic group,  $a_1^-$  is a  $A_1^-$  IR with 3 units of electric flux and  $b_2^+$  is a  $B_2^+$  representation of  $\mathcal{D}_{4h}$  with one unit of electric flux.

$g = 1.4$					
state	a=0.6	a = 0.3	a = 0.15	a = 0	cont.
$\epsilon$	0.2270(3)	0.2034(6)	0.1973(10)	0.1954(6)	0.195
$\epsilon_2$	0.480(3)	0.430(5)	0.418(3)	0.414(2)	0.416
$\epsilon_3$	0.787(6)	0.709(9)	0.689(10)	0.683(8)	0.686
$A_1^+$	1.35(6)	1.40(5)	1.52(3)	1.51(3)	1.509
$E^+$	1.323(6)	1.337(10)	1.363(10)	1.356(8)	1.354
$T_2^+$	2.552(15)	2.52(3)		2.51(4)	2.523
$b_2^+$	0.859(3)	0.950(10)	0.999(7)	1.002(7)	1.007
$A_1^-$	5.42(15)	5.5(2)	5.52(5)	5.53(5)	5.479
$a_1^-$	6.08(10)	6.1(2)		6.1(3)	
$g = 1.8$					
state	a=0.6	a = 0.3	a = 0.15	a = 0	cont.
$\epsilon$	0.523(1)	0.507(2)	0.506(3)	0.503(2)	0.503
$\epsilon_2$	1.133(4)	1.103(6)	1.098(15)	1.094(7)	1.095
$\epsilon_3$	1.92(2)	1.86(3)	1.86(3)	1.85(3)	1.859
$A_1^+$	2.43(5)	2.50(5)	2.56(10)	2.54(6)	2.509
$E^+$	2.27(1)	2.254(10)	2.27(2)	2.255(10)	2.258
$T_2^+$	4.46(4)	4.39(5)	4.35(7)	4.36(5)	4.350
$b_2^+$	1.338(5)	1.380(5)	1.388(10)	1.393(6)	1.386
$A_1^-$	5.92(4)	5.98(3)	6.02(4)	6.01(3)	5.987
$a_1^-$	8.6(2)	8.4(1)	8.3(2)	8.3(2)	
$g = 2.0$					
state	a=0.6	a = 0.3	a = 0.15	a = 0	cont.
$\epsilon$	0.7442(10)	0.7312(15)	0.727(3)	0.727(3)	0.728
$\epsilon_2$	1.621(7)	1.588(10)	1.577(10)	1.575(8)	1.586
$\epsilon_3$	2.72(2)	2.69(3)	2.67(3)	2.67(3)	2.672
$A_1^+$	3.15(15)	3.30(10)	3.1(2)	3.27(15)	3.177
$E^+$	2.879(10)	2.884(15)	2.84(3)	2.87(2)	2.864
$T_2^+$	5.54(10)	5.56(5)	5.49(7)	5.53(5)	5.513
$b_2^+$	1.642(5)	1.657(10)	1.62(3)	1.656(15)	1.660
$A_1^-$	6.05(2)	6.08(3)		6.09(4)	6.113
$a_1^+$	10.2(3)	10.3(2)	10.1(2)	10.2(2)	9.79



would like to thank B. Berg for comments on the manuscript.

## References

- [1] J. Koller and P. van Baal, Nucl. Phys. B302 (1988) 1.
- [2] J. Kripfganz and C. Michael, Nucl. Phys. B314 (1988) 25.
- [3] C. Michael, Nucl. Phys. B329 (1990) 225.
- [4] P. van Baal, Nucl. Phys. B351 (1991) 183.
- [5] P. van Baal, talk presented at the workshop *Frontiers in Nonperturbative Field Theory*, Eger, Hungary, Aug 18-23, 1988. Eds. Z. Horvath, L. Palla, A. Patkos, World Scientific.
- [6] H. Tiedemann, Phys. Rev. D44 (1991) 1280.
- [7] William H. Press et. al: Numerical Recipes, Cambridge University press.
- [8] P. van Baal, Phys. Lett. B224 (1989) 397.